A New Frequency Detector for Orthogonal Multicarrier Transmission Techniques

Flavio Daffara and Ottavio Adami

Laboratoires d'Electronique Philips
22 avenue Descartes, 94453 Limeil-Brévannes Cedex, France
Tel.: +33 1 45.10.67.11 - Fax: +33 1 45.10.69.60
e-mail: daffara@lep-philips.fr

Abstract—This paper deals with the carrier frequency synchronization of orthogonal multicarrier systems, which are an effective transmission technique for coping with the typical channel impairments present in mobile reception. A new carrier frequency detector is introduced and its performance thoroughly analyzed in the presence of a multipath channel. In particular we have analytically derived the frequency detector characteristic curve and its noise power spectral density. We have compared the new algorithm with other known algorithms and we have shown that it permits a considerable improvement in the noise level to be achieved.

I. Introduction

The orthogonal multicarrier (MC) transmission technique, also known as Orthogonal Frequency Division Multiplexing (OFDM) [1], is an effective means of coping with the typical channel impairments present in mobile reception. In fact, MC techniques provide a good protection against the effects of severe multipath propagation, cochannel interference and impulsive parasitic noise, such as occur in digital mobile channels [2-3]. Moreover, thanks to the improvements in digital signal processing, MC systems have become practical to implement and are used for both mobile and fixed applications such as digital audio broadcasting (DAB) [4] and subscriber line modems (ADSL) [5]. The OFDM technique is also proposed for the broadcasting of digital television in Europe [6]. The main feature of OFDM is that the use of an appropriate guard interval eliminates intersymbol interference (ISI) at the sampling time even in the presence of a multipath channel [3].

One of the fundamental functions of an OFDM receiver is the carrier frequency synchronization. Indeed, a residual frequency error between the transmitter and receiver local oscillators leads to a loss of orthogonality between the different subcarriers making up the OFDM signal, thus giving rise to a degradation in the overall system performance [7].

Usually, the frequency error is corrected by using tracking loops in which a frequency detector (FD) provides an estimate of the frequency error to be compensated for. Up to now, the FDs used for OFDM systems were based on the analysis of the signal at the output of the Fast Fourier Transform (FFT) at the receiver side [8-9] (position B in Fig. 1).

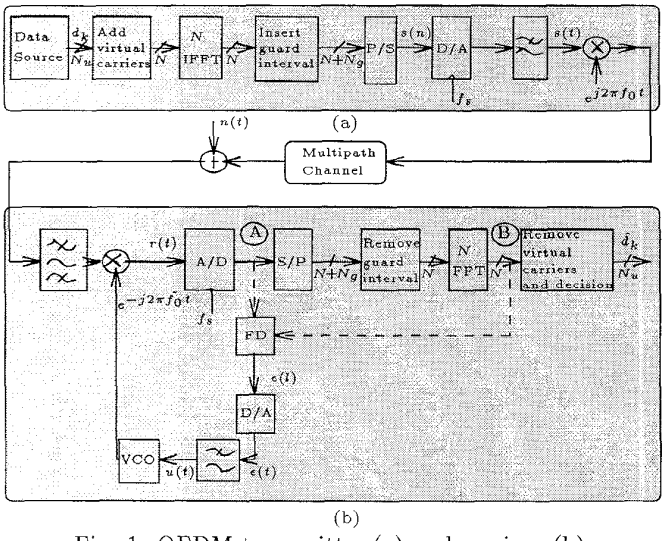

Fig. 1: OFDM transmitter (a) and receiver (b).

These algorithms can be divided into two categories:
1. Algorithms based on the analysis of special synchronization blocks embedded in the OFDM temporal frame (an example can be found in [8]).
2. Algorithms based on the analysis of the received data at the output of the FFT (an example can be found in [9]).

The first category of algorithms presents, however, some drawbacks. Mainly such algorithms have a long acquisition time due to the fact that in an OFDM temporal frame there are only a few special synchronization blocks every many data blocks. Moreover, they require quite a high computational complexity in order to get rid of nonlinearity problems and multipath channel effects. On the contrary, the second category of algorithms does not need any special blocks but gives poor results in the presence of a multipath propagation (which is the case of OFDM applications in mobile radio channels).

In this paper we introduce a new carrier frequency error

0-7803-2742-X/95 $4.00 © 1995 IEEE

detector able to overcome these drawbacks. Such a FD is based on the analysis of the sampled received signal before the FFT block (position A in Fig. 1) and makes use of the redundancy introduced by the insertion of the guard interval in the OFDM technique.

The paper is organized as follows: after a description of the considered transmission system in Section II, we present the model of the multipath channel used in our simulations in Section III. The new frequency detector is introduced in Section IV and its open loop and closed loop performance are given in Section V and Section VI respectively. Finally, Section VII is for our conclusions.

II. System Description

The considered transmission system is based on an orthogonal frequency division multiplexing technique [1-3]. The principle of this multiplexing technique consists in having a large number N_u of modulated carriers (each carrying a low bit rate) which are summed for transmission (frequency multiplexing). For maximum spectral efficiency, an overlapping in the spectra of the emitted carriers is tolerated: in this case an orthogonality condition on the subcarrier frequencies guarantees the absence of cross-talk between modulated subcarriers at the sampling time. The OFDM makes use of an N-point FFT algorithm for multiplexing ($N > N_u$). $N - N_u$ subcarriers are not used to ensure sufficiently wide filter guard bands. Moreover, because of the multipath environment, a guard interval (T_g) is inserted at the beginning of each transmitted block [3]. The length of T_g should be greater than the multipath spread (T_m) [10] in order to prevent intersymbol interference within the OFDM block. Typical values of T_m are $T_m = 0.7$ μs for rural terrain, $T_m = 7$ μs for urban terrain and $T_m = 100$ μs for mountain terrain [11].

Fig. 1 shows the block diagram of an OFDM transmission system. Let us consider a system with N_u useful carriers frequency-spaced by $1/T$. Every $T' = T + T_g$ seconds a block of N_u data is generated from the data source. After the addition of $N - N_u$ null data corresponding to the virtual carriers at the edges of the spectrum, the obtained N samples are processed by an Inverse Fast Fourier Transform (IFFT) of size N and a guard interval (cyclic prefix) made up with the last N_g samples is added at the beginning of each block. The $N + N_g$ samples generated during the l^{th} block ($lT' \leq t \leq (l+1)T'$) are therefore equal to

$$s(n) = \frac{1}{\sqrt{N}} \sum_{k=0}^{N-1} d_k(l) e^{j2\pi \frac{kn}{N}} \quad \text{for} \quad -N_g \leq n \leq N-1, \qquad (1)$$

where the data $d_k(l)$ are independent and identically distributed (iid) MxM-QAM constellation symbols of variance σ_d^2. After a Parallel-to-Serial (P/S) and a Digital-to-Analog (D/A) conversion we obtain the baseband transmitted signal $s(t)$ which is up-converted at the carrier frequency f_0.

The received signal is filtered by a band-pass filter of bandwidth $\frac{N}{T}$, which selects the desired signal. After the A/D converter (at a sampling frequency $f_s = \frac{N}{T}$) the first N_g samples of each incoming block are removed. The vector of the N useful samples then enters a Fast Fourier Transform (FFT) processor whose output provides the received data. In the sequel we will consider an OFDM system with the following parameters: $N = 2048$, $N_u = 1705$, $f_s = 9$ MHz, $T_g = 0.125T$ and $T' = 256$ μs.

In the presence of a frequency offset $\Delta f = f_0 - \tilde{f}_0$ between the transmitter oscillator and the receiver one, the baseband received signal can be written as $r(t) = s(t)e^{j2\pi\Delta f t}$. Fig. 1 shows also the Phase-Locked Loop (PLL) for the correction of Δf. The frequency detector produces an error signal $\epsilon(l)$ whose average value is proportional to the frequency error between the carrier frequency of the incoming signal and the frequency generated by the Voltage Controlled Oscillator (VCO). The signal $u(t)$ at the output of the low-pass loop filter is linearly related, through a gain factor K_0, to the VCO frequency. When the loop is locked, this frequency is equal on average to f_0 and the received signal is correctly demodulated. In an OFDM transmission system the carrier synchronization is a very important function since the presence of a frequency error Δf causes a degradation of the performance. Fig. 2 shows the plot of the Signal-to-Noise Ratio (SNR) degradation at a Symbol Error Rate (SER) of 10^{-4} due to a frequency offset ΔfT. The use of efficient algorithms for the carrier recovery is therefore a crucial point in the design of an OFDM receiver.

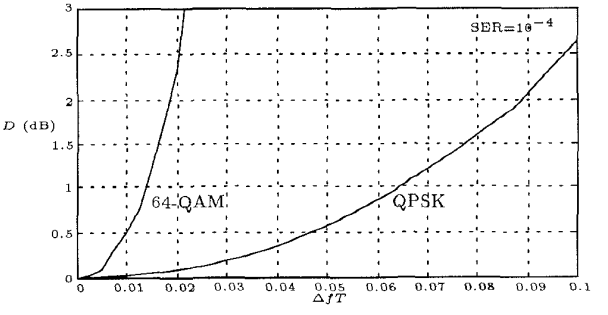

Fig. 2: Degradation due to a frequency offset (SER=10^{-4}).

III. Multipath Channel Model

In the case of a multipath channel, the baseband received signal can be written as [10]

$$r(t) = \sum_{n=1}^{N_p} \rho_n(t) s[t - \tau_n(t)], \qquad (2)$$

where $s(t)$ is the baseband transmitted signal, N_p is the number of paths, $\rho_n(t)$ and $\tau_n(t)$ are respectively the complex attenuation and the delay associated with the n^{th} path. Generally the attenuation and the delay of each ray are time-variant. Let be B_d the doppler spread of the channel [10]. In the case of a mobile receiver the doppler spread (i.e. the maximum doppler frequency) is equal to $B_d = \frac{v}{c} f_0$, where v (resp. c) is the mobile (resp. light) speed and f_0 is the carrier frequency. By assuming a carrier frequency of 500 MHz and a maximum mobile speed of 200 km/h we have $B_d \simeq 92$ Hz, which gives a channel coherence time [10] $T_c = 1/B_d \simeq 10$

ms. This time is large compared to the useful block period ($T \simeq 228\ \mu s$). In the next section we will see that the proposed frequency detector algorithm makes use of couple of samples time-spaced by the useful block duration. Therefore the channel can be considered stationary with respect to the algorithm and in the sequel we will neglect the time-variance of the channel. When the number N_p of paths is sufficiently large, the received signal $r(t)$ is a zero-mean complex Gaussian random process. Thus the modulus of $r(t)$ follows a Rayleigh distribution and its phase is uniformly distributed between 0 and 2π. In our simulations we have used a multipath channel derived from a typical channel profile of a urban, non hilly terrain [11] with $N_p = 20$ rays. For each ray, a random delay distributed according to a negative exponential law, a random phase uniformly distributed between 0 and 2π and a Rayleigh-distributed random attenuation have been drawn. Table 1 gives the amplitude, phase and delay of each ray. The corresponding time-discrete channel model has

Ray	delay [μs]	modulus	phase [rad]
1	1.0030	0.0576	4.8550
2	5.4221	0.1768	3.4191
3	0.5186	0.4071	5.8645
4	2.7518	0.3036	2.2159
5	0.6029	0.2588	3.7581
6	1.0166	0.0618	5.4302
7	0.1436	0.1503	3.9520
8	0.1538	0.0515	1.0936
9	3.3249	0.1850	5.7752
10	1.9356	0.4001	0.1545
11	0.4300	0.2957	5.9284
12	3.2289	0.3508	3.0530
13	0.8488	0.2629	0.6286
14	0.0739	0.2259	2.1285
15	0.2039	0.1710	1.0995
16	0.1942	0.1497	3.4630
17	0.9244	0.2401	3.6648
18	1.3813	0.1166	2.8338
19	0.6406	0.2212	3.3343
20	1.3687	0.2597	0.3939

Table 1: Multipath channel model: drawing of 20 paths corresponding to the COST-207 urban, non hilly profile [11].

been drawn in Fig. 3. Coefficients c_i have been evaluated by

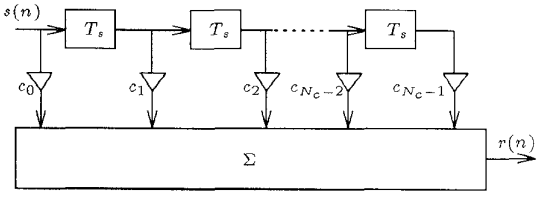

Fig. 3: Time-discrete model of the channel.

imposing the same channel frequency response (within the signal bandwidth) between the analog and the time-discrete channel. Fig. 4 shows the modulus of the frequency response of the considered channel.

IV. Guard-Interval-Based FD

In this section we propose a new algorithm for the carrier recovery in an OFDM receiver. Fig. 5 shows the samples r_n $(-N_g \leq n \leq N-1)$ of the received baseband signal $r(t)$ belonging to the l^{th} block. The first N_g samples of the block $(-N_g \leq n \leq -1)$ belong to the guard interval, while the

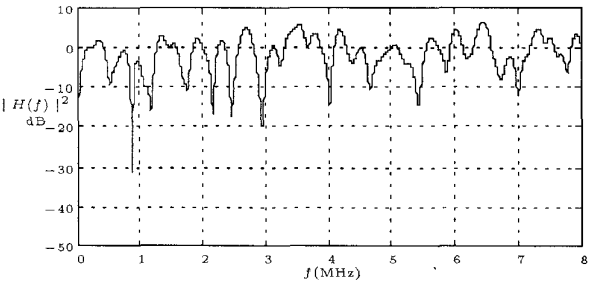

Fig. 4: Multipath channel model: frequency response.

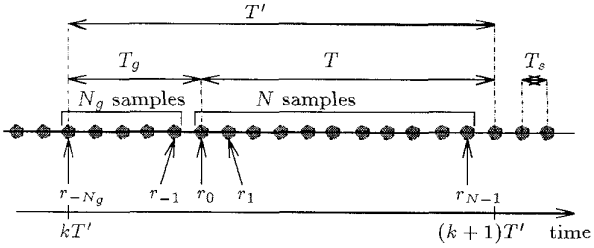

Fig. 5: Temporal order of the transmitted samples within an OFDM block.

other N samples $(0 \leq n \leq N-1)$ represent the useful block. The new FD algorithm uses the redundancy introduced by the guard interval. Let us consider the case of an additive white Gaussian noise (AWGN) channel. When the frequency error Δf is null, we have $r_{N-i} = r_{-i}$ $(i = 1, 2, ..., N_g)$ and therefore the product $r_{N-i}r^*_{-i}$ is a real number. However, in the presence of a frequency error the two samples r_{N-i} and r^*_{-i} are affected by a different rotation and the imaginary part of their product contains some information about the frequency offset. The basic idea of the new algorithm is to use this information. The error signal $\epsilon(l)$ corresponding to the l^{th} block is given by

$$\epsilon(l) = \frac{1}{L}\sum_{i=1}^{L} \text{Im}[r_{N-i}r^*_{-i}] \quad \text{with} \quad 1 \leq L \leq N_g, \tag{3}$$

where Im is the function taking the imaginary part of a complex number and L the number of guard interval samples taken into account. In the sequel we will refer to this algorithm as the Guard-Interval-Based (GIB) algorithm.

V. Open Loop Analysis

In this section we analyse the performance of the algorithm in the presence of a multipath channel. Let us assume that the channel impulse response has a duration of N_cT_s. It can be shown [3] that if $N_c < N_g$ then the only channel effect is to multiply the received data on the k^{th} subcarrier by the channel frequency response evaluated at the frequency $\frac{k}{T}$. Therefore the received signal in the l^{th} block is equal to

$$r(n) = \frac{1}{\sqrt{N}} \sum_{k=0}^{N-1} d_k(l) H_k e^{j2\pi \frac{kn}{N}} e^{j2\pi \Delta f T' l} e^{j2\pi \Delta f T \frac{n}{N}} + n(lT' + nT_s) \tag{4}$$

if $-(N_g - N_c) \leq n \leq N-1$, where H_k is the value of the channel frequency response at the frequency $f_k = \frac{k}{T}$ and

$n(t)$ the noise at the output of the band-pass filter. Assuming that the channel introduces complex AWGN with a two-sided spectral density $2N_0$ and that the filter has a rectangular bandwidth of $\frac{N}{T} = \frac{1}{T_s}$, the autocorrelation function of $n(t)$ is equal to

$$R_n(\tau) = E[n(t+\tau)n^*(t)] = 2N_0 \frac{N}{T} \frac{\sin(\tau/T_s)}{\tau/T_s}. \quad (5)$$

From expression (5) we obtain

$$R_n(iT_s) = \begin{cases} 2N_0 \frac{N}{T} = \sigma_n^2 & \text{if } i = 0 \\ 0 & \text{elsewhere,} \end{cases} \quad (6)$$

where σ_n^2 is the noise variance. Let us assume that the last L samples of the guard interval are not affected by the channel echoes, i.e. $N_c < N_g - L$. This assumption is not restrictive for small values of L since normally the guard interval is chosen longer than the expected channel impulse response duration. Substituting expression (4) into equation (3) leads to the expression of the error signal in the case of a multipath channel:

$$\epsilon(l) = \frac{1}{LN} \sum_{i=1}^{L} \mathrm{Im} \left[\sum_{k=0}^{N-1} \sum_{k'=0}^{N-1} d_k(l) d_{k'}^*(l) H_k H_{k'}^* e^{-j2\pi \frac{k-k'}{N} i} e^{j2\pi \Delta f T} \right]$$
$$+ \frac{1}{L\sqrt{N}} \sum_{i=1}^{L} \mathrm{Im} \left\{ n[lT' + (N-i)T_s] \sum_{k'=0}^{N-1} d_{k'}^*(l) H_{k'}^* e^{j2\pi \frac{k'}{N} i} e^{-j2\pi \Delta f T' l} e^{j\frac{2\pi}{N} \Delta f T i} \right.$$
$$\left. + n^*(lT' - iT_s) \sum_{k=0}^{N-1} d_k(l) H_k e^{-j2\pi \frac{k}{N} i} e^{j2\pi \Delta f T' l} e^{j\frac{2\pi}{N} \Delta f T (N-i)} \right\}$$
$$+ \frac{1}{L} \sum_{i=1}^{L} \mathrm{Im}\{n[lT' + (N-i)T_s] n^*[lT' - iT_s]\}. \quad (7)$$

A. Characteristic Curve

Now let us evaluate the characteristic curve of the FD algorithm. Since the data on the different carriers are independent and identically distributed and using expression (6) the average of expression (7) becomes

$$E[\epsilon(l)] = g(\Delta f) = \frac{\sigma_d^2}{N} \sin(2\pi \Delta f T) \sum_{k \in \mathcal{K}} |H_k|^2, \quad (8)$$

where $\mathcal{K}$ is the set of index k corresponding to the useful carriers, i.e. $k \in \mathcal{K}$ if $\lfloor \frac{N-N_u}{2} \rfloor \leq k \leq \lfloor \frac{N-N_u}{2} \rfloor + N_u - 1$. From this expression we can see that the only channel effect is to modify the amplitude of the characteristic curve. It is important to notice that, even if the channel introduces severe fading, it does not change the position of the zeros of $g(\Delta f)$, i.e. it does not introduce any bias in the frequency estimation. Fig. 6 shows the characteristic curve of the GIB FD for an OFDM system with N=2048, $N_u = 1705$ and $T_g = 0.125T$. We can see that the algorithm has an acquisition range of $-0.5 \leq \Delta f T \leq 0.5$.

By taking the derivative of expression (8) with respect to Δf and evaluating it for $\Delta f = 0$, we obtain the gain of the proposed algorithm, which is equal to

$$K_d = \frac{\sigma_d^2}{N} 2\pi T \sum_{k \in \mathcal{K}} |H_k|^2. \quad (9)$$

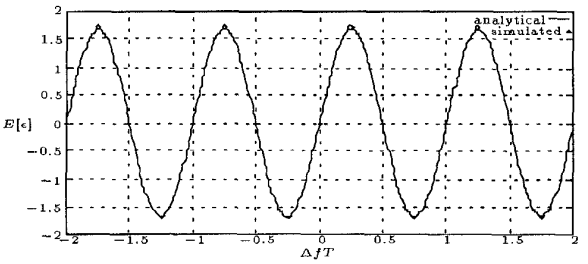

Fig. 6: Characteristic curve of the GIB FD for an OFDM system with N=2048, $N_u = 1705$ and $T_g = 0.125\,T$.

B. Power Spectral Density

Let us split the error signal in the sum of its mean value and a random zero-meaned noise term:

$$\epsilon(l) = E[\epsilon(l)] + \nu(l). \quad (10)$$

From expression (7), we can see that the noise $\nu(l)$ is made up of three terms:

1. a term due to the signal-to-signal interaction (this term is also known as pattern or self noise)

$$\nu_{SS}(l) \triangleq \frac{1}{LN} \sum_{i=1}^{L} \mathrm{Im} \left[\sum_{k=0}^{N-1} \sum_{k' \neq k} d_k(l) d_{k'}^*(l) H_k H_{k'}^* e^{-j2\pi \frac{k-k'}{N} i} e^{j2\pi \Delta f T} \right]; \quad (11)$$

2. a term due to the signal-to-noise interaction

$$\nu_{SN}(l) \triangleq \frac{1}{L\sqrt{N}} \sum_{i=1}^{L} \mathrm{Im} \left\{ n[lT' + (N-i)T_s] \sum_{k'=0}^{N-1} d_{k'}^*(l) H_{k'}^* e^{j\frac{2\pi i}{N}(k' + \Delta f T)} e^{-j2\pi \Delta f T' l} \right.$$
$$\left. + n^*(lT' - iT_s) \sum_{k=0}^{N-1} d_k(l) H_k e^{-j2\pi \frac{k}{N} i} e^{j2\pi \Delta f T' l} e^{j\frac{2\pi}{N} \Delta f T (N-i)} \right\}; \quad (12)$$

3. a term due to the noise-to-noise interaction

$$\nu_{NN}(l) \triangleq \frac{1}{L} \sum_{i=1}^{L} \mathrm{Im}\{n[lT' + (N-i)T_s] n^*[lT' - iT_s]\}. \quad (13)$$

Since ν_{SS}, ν_{SN} and ν_{NN} are uncorrelated stationary random processes, the power spectral density of $\nu(l)$ is given by

$$S_\nu(f) = S_{SS}(f) + S_{SN}(f) + S_{NN}(f), \quad (14)$$

where $S_{SS}(f)$, $S_{SN}(f)$ and $S_{NN}(f)$ are the power spectral densities of $\nu_{SS}(l)$, $\nu_{SN}(l)$ and $\nu_{NN}(l)$ respectively.

We are interested in evaluating the statistical properties of $\nu(l)$ when the frequency recovery PLL is in its steady state, i.e. when $\Delta f = 0$. To evaluate $S_{SS}(f)$ let us consider expression (4) with $\Delta f = 0$ and without the noise. It can be observed that $r_{N-i} = r_{-i}$. The product $r_{N-i} r_{-i}^*$ is therefore a real number and its imaginary part is identically null. Indeed we have $\nu_{SS}(l) = 0\ \forall l$, i.e. $S_{SS}(f) = 0\ \forall f$. This means that the algorithm has no self-noise when $\Delta f = 0$.

The expressions of $S_{SN}(f)$ and $S_{NN}(f)$ have been calculated, but the derivations will be not reported here for brevity. The results are:

$$S_{SN}(f) = \frac{1}{T^2} \frac{1}{L} \frac{N}{N_u} \frac{1}{4\pi^2 \gamma} K_d^2 \quad (15)$$

and

$$S_{NN}(f) = \frac{1}{T^2}\frac{1}{L}\left(\frac{N}{N_u}\right)^2 \frac{1}{8\pi^2\gamma^2}K_d^2, \tag{16}$$

where γ is the average SNR at the FFT output given by

$$\gamma = \frac{1}{N_u}\frac{\sigma_d^2}{\sigma_n^2}\sum_{k\in\mathcal{K}} \mid H_k \mid^2 . \tag{17}$$

It is important to notice that the power spectral density is constant with respect to the frequency. Fig. 7 shows the plots of the normalized power spectral densities of ν_{SN} and ν_{NN} as function of γ.

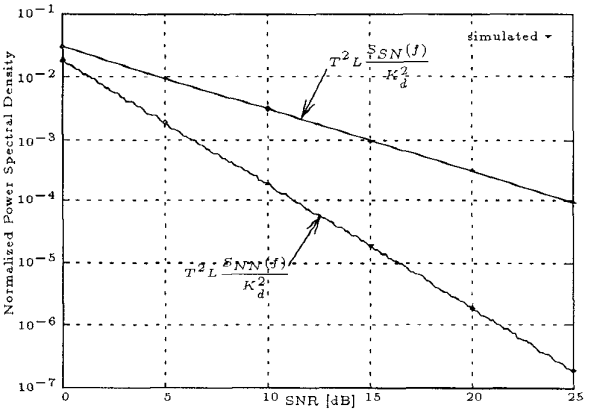

Fig. 7: Normalized power spectral densities of ν_{SN} and ν_{NN} for $N = 2048$ and $N_u = 1705$.

VI. Closed Loop Analysis

The frequency recovery loop equivalent digital model valid for the frequency variations [12] is depicted in Fig. 8, where $f(l)$ represents the input frequency, $\tilde{f}(l)$ the VCO output frequency, K_0 the equivalent model VCO gain factor and $G(z)$ the digital loop filter transfer function given by

$$G(z) = \frac{K_1 z^{-1}}{1 - z^{-1}}, \tag{18}$$

where K_1 is the filter gain.

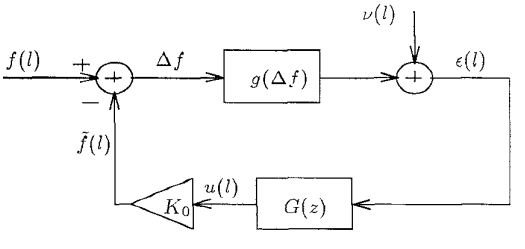

Fig. 8: Frequency recovery loop digital equivalent model valid for frequency variations.

Since we are interested in studying the steady-state frequency jitter, the loop can be considered near its equilibrium point and we can make the following assumption:

$$g(\Delta f) = K_d \Delta f. \tag{19}$$

Fig. 9 shows the block diagram of the linearized loop whose closed loop transfer function is equal to

$$H(z) = \frac{K_d K_0 K_1}{z - 1 + K_d K_0 K_1}. \tag{20}$$

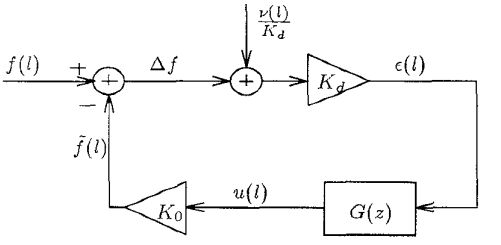

Fig. 9: Frequency recovery loop linearized equivalent model valid for frequency variations.

It can be shown [12] that the steady-state frequency jitter $\sigma_{\Delta f}^2$ at the output of the VCO is equal to

$$\sigma_{\Delta f}^2 = T' \int_{-\frac{1}{2T'}}^{\frac{1}{2T'}} \frac{S_\nu(f)}{K_d^2} \mid H(e^{j2\pi f T'}) \mid^2 df. \tag{21}$$

Since $S_\nu(f)$ is constant, expression (21) becomes

$$\sigma_{\Delta f}^2 = \frac{S_\nu(0)}{K_d^2} 2 B_L T', \tag{22}$$

where B_L is the PLL noise bandwidth defined as [12]

$$B_L = \int_0^{\frac{1}{2T'}} \mid H(e^{j2\pi f T'}) \mid^2 df. \tag{23}$$

A. Steady-State Frequency Jitter

By using expressions (15) and (16) we obtain the relationship between $\frac{S_\nu(0)}{K_d^2}$ and the average SNR γ:

$$\frac{S_\nu(0)}{K_d^2} = \frac{1}{T^2}\frac{1}{L}\frac{N}{N_u}\frac{1}{4\pi^2\gamma}\left[1 + \frac{N}{N_u}\frac{1}{2\gamma}\right]. \tag{24}$$

Substituting expression (24) into equation (22) we obtain the normalized frequency jitter, which is equal to

$$\sigma_{\Delta f T}^2 = \frac{1}{L}\frac{N}{N_u}\frac{1}{2\pi^2\gamma}\left[1 + \frac{N}{N_u}\frac{1}{2\gamma}\right] B_L T'. \tag{25}$$

It has to be noticed that the frequency jitter is a decreasing function of L. However, the value of L cannot be chosen too large since in that case the guard-interval points could be affected by the channel impulse response. The frequency jitter could also be decreased by decreasing the PLL bandwidth, but in this case a higher acquisition time is obtained. Fig. 10 shows the comparison between the normalized power spectral density of the GIB algorithm and the power spectral density of two other frequency estimation algorithms: the AFC algorithm [8] and the Maximum-Likelihood (ML) estimator [9]. The considered constellation is a QPSK with $\frac{E_s}{N_0} = 8$ dB where E_s is the energy per transmitted symbol. The GIB algorithm power spectral density does not depend on the number of carriers and we can see that this algorithm

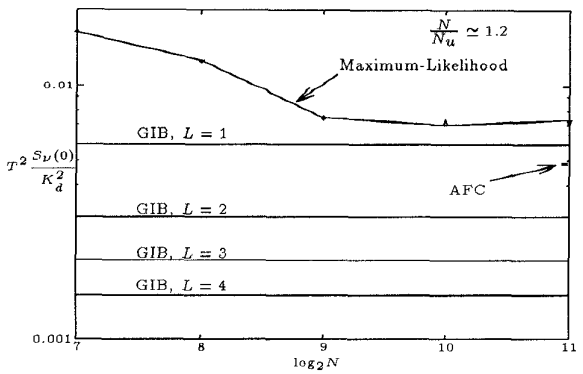

Fig. 10: Comparison between the normalized power spectral densities of the GIB algorithm, the ML algorithm and the AFC algorithm in the case of QPSK with $\frac{E_s}{N_0} = 8$ dB.

outperforms the AFC one if L is at least equal to 2. Concerning the ML algorithm, $\frac{S_\nu(0)}{K_d^2}$ decreases linearly with the number of carriers because the error signal is obtained by averaging over all the useful carriers reducing therefore the noise effect. However, the ML algorithm is worse than the GIB one for the commonly used FFT sizes.

B. Acquisition Time

We have also carried out some computer simulations to evaluate the acquisition time of the proposed algorithm in the presence of the multipath channel described in Section III. We have assumed an initial frequency offset $\Delta f = \frac{0.5}{T}$, which corresponds to the upper limit of the acquisition range and we have considered a QPSK with $\frac{E_s}{N_0} = 8$ dB. The value of γ to be used is therefore $\gamma = 7.488$ dB since the use of the guard interval leads to a SNR loss of about 0.5 dB (10 $\log_{10}(1 + T_g/T)$). The values of the PLL bandwidth have been chosen to have a constant steady-state frequency jitter for different values of L. In particular we have taken $\sigma^2_{\Delta fT} = 10^{-4}$, which gives rise to a negligible degradation (see Fig. 2). Fig. 11 shows the acquisition time for the QPSK. It can be

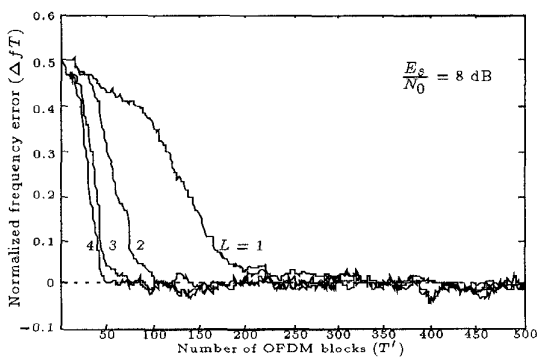

Fig. 11: Acquisition time for an OFDM system with $N = 2048$, $N_u = 1705$ and $T_g = 0.125T$ (QPSK transmission in multipath channel).

observed that the acquisition time is a decreasing function of L. In fact, when L increases, we can choose a higher value of the bandwidth (which results in faster acquisition) to obtain the wanted value of frequency jitter.

VII. Conclusions

In this paper we have introduced a new frequency detector for orthogonal multicarrier systems. Such a frequency detector is particularly simple to implement and does not require any special synchronization blocks embedded in the data temporal frame. We have compared its performance with other known algorithms and we have found that it achieves a considerable improvement in the noise level. After a detailed analysis in the presence of a multipath channel, we have shown that the proposed algorithm is a valid candidate for carrier frequency recovery in applications employing OFDM transmission techniques.

References

[1] J.A. Bingham, *Multicarrier Modulation for Data Transmission: an idea whose time has come*, IEEE Commun. Mag., pp. 5-14, May 1990.

[2] L.C. Cimini, Jr., *Analysis and Simulation of a Digital Mobile Channel Using Orthogonal Frequency-Division Multeplixing*, IEEE Trans. Commun., vol. COM-33, n.7, pp. 665-675, July 1985.

[3] M. Alard and R. Lassalle, *Principles of modulation and channel coding for digital broadcasting for mobile receiver*, EBU Review, n. 224, pp. 3-25, August 1987.

[4] B. Le Floch, R. Halbert-Lassalle, D. Castelain, *Digital Sound Broadcasting to Mobile Receivers*, IEEE Trans. Consum. Electr., vol. 35, n. 3, pp. 493-503, August 1989.

[5] W.Y. Chen and D.L. Waring, *Applicability of ADSL to Support Video Dial Tone in the Copper Loop*, IEEE Commun. Mag., pp. 102-109, May 1994.

[6] P.G.M. de Bot, B. Le Floch, V. Mignone and H.-D. Schütte, *An Overview of the Modulation and Channel Coding Schemes Developed for Digital Terrestrial Television Broadcasting within the dTTb Project*, International Broadcasting Convention, Amsterdam, The Netherlands, September 1994.

[7] H. Sari, G. Karam and I. Jeanclaude, *Channel Equalization and Carrier Synchronization in OFDM Systems*, Conf. Rec. of 6th Int. Tirrenia Workshop on Digital Communications, Tirrenia, Italy, September 1993.

[8] N. Philips and L. Jeanne, *System for Broadcasting and Receiving Digital Data, Receiver and Transmitter for Use in such System*, International Patent, Application Number: PCT/NL92/00039, February 1992.

[9] F. Daffara and A. Chouly, *Maximum Likelihood Frequency Detectors for Orthogonal Multicarrier Systems*, Conf. Rec. of IEEE International Conference on Communications ICC'93, pp. 766-771, Geneva, Switzerland, May 23-26, 1993.

[10] J.G. Proakis, *Digital Communications*, McGraw-Hill, 1989., published by the Commission of the European Communities, Brussels, Luxembourg, 1989.

[11] *Digital Land Mobile Radio Communications* - COST 207, published by the Commission of the European Communities, Brussels, Luxembourg, 1989.

[12] H. Meyr and G. Ascheid, *Synchronization in Digital Communications*, Vol. 1, John Wiley & Sons, 1990.